

Assessing Intermolecular Interactions in Guest-Free Clathrate Hydrate Systems

Iván León-Merino[§], Raúl Rodríguez-Segundo[§], Daniel J. Arismendi-Arrieta[§], and
Rita Prosmi^{§*}

[§]*Institute of Fundamental Physics (IFF-CSIC), CSIC, Serrano 123, 28006 Madrid, Spain*

E-mail: rita@iff.csic.es;Phone:+34-91-5616800Ext.941131

*To whom correspondence should be addressed

Abstract

Recently, empty hydrate structures sI, sII, sH and others have been proposed as low-density ice structures by both experimental observations and computer simulations. Some of them have been synthesized in the laboratory, that motivates further investigations on the stability of such guest-free clathrate structures. Using semiempirical and *ab initio*-based water models, as well as dispersion-corrected density functional theory approaches, we predict their stability, including cooperative many-body effects, in comparison with reference data from converged wavefunction-based DF-MP2 electronic structure calculations. We show that large basis sets and counterpoise corrections are required in order to improve convergence in the interaction/binding energies for such systems. Therefore, extrapolation schemes based on triple/quadruple and quadruple/quintuple zeta quality basis sets are used to reach high accuracy. Eleven different water structures corresponding to dodecahedron, edge sharing, face sharing and fused cubes, as a part of the WATER27 database, as well as cavities from the sI, sII and sH clathrate hydrates formed by 20, 24, 28 and 36 water molecules, are employed, and new benchmark energies are reported. Using these benchmark sets of interaction energies, we assess the performance of both analytical models and direct DFT calculations for such clathrate-like systems. In particular, seven popular water models (TIP4P/ice, TIP4P/2005, q-TIP4P/F, TTM2-F, TTM3-F, TTM4-F and MB-pol) available in the literature, and nine density functional approximations (3 meta-GGAs, 3 hybrids and 3 range separated functionals) are used to investigate their accuracy. By including dispersion corrections, our results show that errors in the interaction energies are reduced for most of the DFT functionals. Despite the difficulties faced by current water models and DFT functionals to accurately describe the interactions in such water systems, we found some general trends that could serve to extend their applicability to larger systems.

1. INTRODUCTION

Clathrate hydrates are ice-like non-stoichiometric inclusion compounds with cage-like structures where small molecules, such as H₂, N₂, CH₄, CO₂, .. etc, can be trapped. Such compounds

are naturally formed, and due to their potential technological applications (*e.g.* future energy resource, and gas storage materials), they have received considerable attention in the research community by both experiment and theory.^{1,2} The hydrates are thermodynamically stable when guest molecules occupy the host cages, due to the interactions between the host and guest involving mainly van der Waals (vdW) (noncovalent) interactions.³ More recently, an empty structure of sII clathrate, known as ice XVI, has been stabilized,⁴ as well as a low-density clathrate sIII,⁵ while the existence of virtual ices,⁶ and other low-density structures, namely aereoices,⁷ have been also predicted by computer simulations. The experimental evidence of such guest-free clathrates indicates that water molecules can form low density crystalline phase structure, motivating in this way further investigations on ice clathrate cage-like structures.

Up to now, from the theoretical perspective, the investigations are still ongoing towards the development of fundamental physico-chemical processes in clathrate exploitation, including their microscopic structural evolution, aiming to gain a better understanding of stabilities and storage capacities of their cavities.^{2,8-10} The rapid increase in computing power has also led to numerous quantum chemistry calculations on guest-host interactions, as well as a plethora of benchmark computations in large water clusters.¹¹⁻²¹ The results of such studies have shown that *ab initio* electronic structure methods provide independent and accurate means of reaching a good understanding of the nature of hydrates and description of the underlying guest-host potential.^{16,22,23} For larger molecular systems wavefunction-based methods become computationally more expensive, while more recently different density functional theory (DFT) approaches tend to present a more economical, and at the same time reliable means, for describing noncovalent interactions.^{24,25} In such water systems there is a balance between vdW and hydrogen bond interactions. Widely used DFT functionals are inadequate, as they do not explicitly describe the dispersion effects.²⁴ In particular, for dispersion-dominated complexes a non-localized energy description is required, and modern improved DFT approaches, within the higher rungs of Jacob's ladder, appear being potentially more accurate.²⁵ Numerous ways for overcoming these disadvantages of DFT have been currently reported in the literature.²⁶⁻³⁰ One example is the use of DFT-D methods, which are com-

putationally economical forms to include empirical dispersion corrections to the DFT functionals. The DFT-D3 methods have significant computational cost advantages over more robust and powerful treatment of dispersion methods that explicitly incorporate nonlocal correlation. Thus, a significant amount of work has been already directed toward validating the performance of the DFT-D3 method, which it has been found to be reliable for describing noncovalent interactions.^{31–33}

Numerous *ab initio* studies have investigated the binding energies of various water clusters,^{12,19,20,34–36} ranking the accuracy of DFT functionals, however they have focused primarily on small water clusters, rarely containing more than eight water molecules,¹¹ and just recently new reference data for the interactions energies of water icosamers have been reported.^{16,19,21,35} Given the recent interest in such complexes, and the lack of reference computations motivates us to assess available force fields, and common as well as improved DFT approaches for representing the interactions of such systems with strong cooperative many body effects.

The article is organized as follows: in section 2 we present the specific cavities’ structures introduced in this study, as well as various details of the wave-function and density function theory electronic structure methods employed; in section 3 we present the benchmark results from the DF-MP2 calculations, some of the analytical potential models available in the literature for describing water-water interactions, and from the DFT/DFT-D computations. In turn, through a systematic analysis we evaluate the quality of the underlying interactions within the cavities of sI, sII and sH clathrate hydrates, computed by pairwise semiempirical and pairwise/many-body *ab initio* water model potentials, and by DFT-D3 approaches in comparison with reference converged DF-MP2 data; and in section 4 we summarize our main conclusions.

2. COMPUTATIONAL DETAILS

2.1. Cages’ configurations. The three most common structures of clathrate hydrates are the type I (sI), II (sII) and H (sH).¹ In sI hydrate, the unit cell is formed from small pentagon dodecahedral 5^{12} cavities (with $N=20$ water molecules), and slightly larger (with $N=24$) tetrakaidecahedral $5^{12}6^2$

cages, sII contains 5^{12} and $5^{12}6^4$ hexakaidecahedron (with $N=28$), while sH has pentagon 5^{12} and irregular ($4^35^66^3$) dodecahedron (also with $N=20$), as well as icosahedron $5^{12}6^8$ (with $N=36$) cavities. While the positions of oxygen atoms in water molecules have been experimentally determined by X-ray diffraction analysis of clathrate hydrate structures, the positions of water hydrogen atoms in the lattice are disordered.

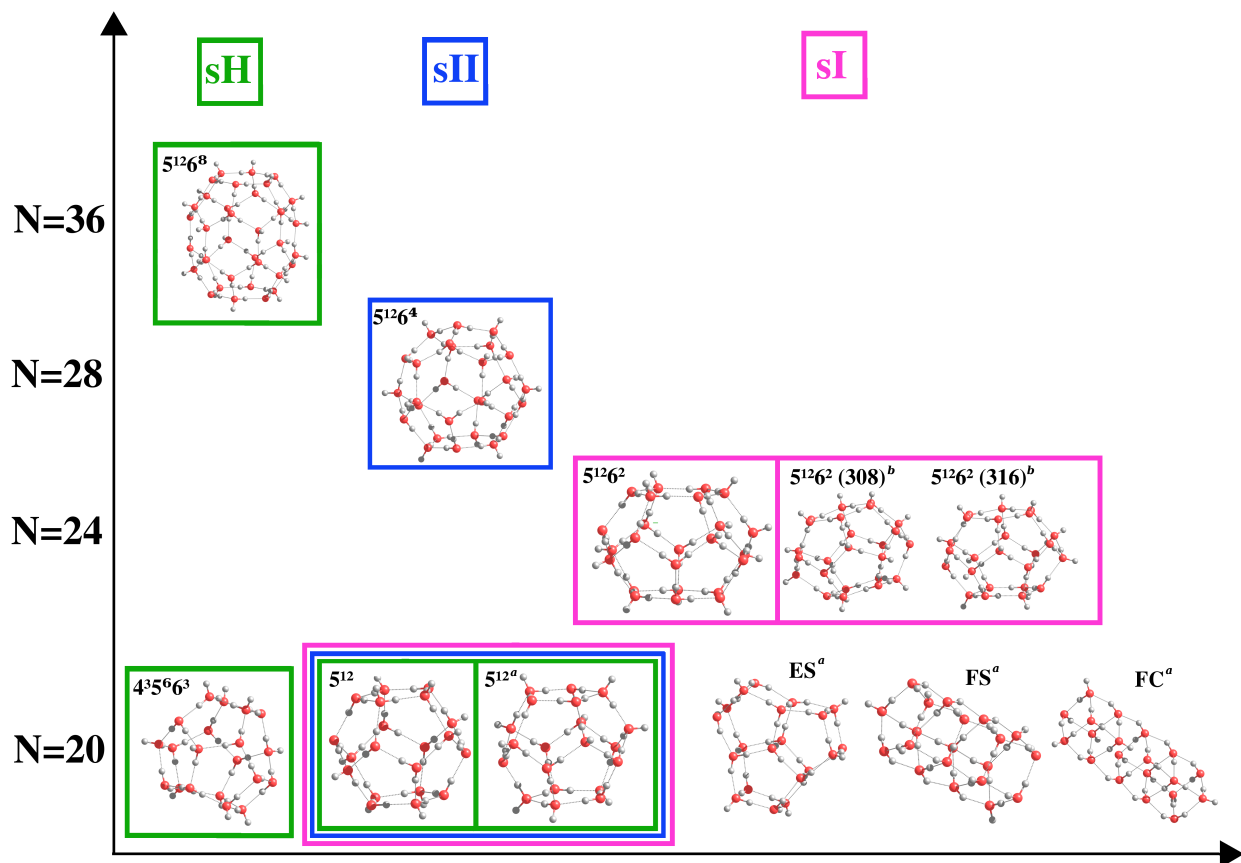


Figure 1: The cage structures of the sI (magenta color), sII (blue color) and sH (green color) clathrate hydrates, as well as the 5^{12a} , ES^a , FC^a and FS^a , and 308^b , 316^b water structures used in this study (see text).

Therefore, we extracted geometries for all cages in the sI, sII and sH clathrates from the 3D crystalline frameworks, as they have been determined in Ref.³⁷ satisfying the ice rules, having the lowest potential energy configuration for the protons, and a net zero dipole moment. In addition to the above geometries, for the $(H_2O)_{20}$ system we also used in the present study, four structures for the WATER27 data set¹¹ corresponding to the B3LYP/6-311++G(2d,2p) optimized geometries of the dodecahedral, edge-sharing (ES), fused-cubes (FC), and face-sharing (FS) structures.³⁸ For

the (H₂O)₂₄ cage we also provide data for configurations of previous studies,^{13,39} while, to our knowledge, no other benchmark data have thus far been reported for the (H₂O)₂₈ and (H₂O)₃₆ cages.

All structures used in this work are displayed in Fig. 1, while the geometries of the newly introduced structures are given in the Supporting Information. In particular, for N=20 we show 6 structures, namely 4³5⁶6³, 5¹², 5^{12a}, ES^a, FS^a, and FC^a (^a stands for structures from Ref.¹¹), for N=24 we list 3 structures, the 5¹²6², 308^b and 316^b (with ^b indicated structures from Ref.³⁹), while for N=28 and N=36 we consider one structure for each of them, namely 5¹²6⁴ and 5¹²6⁸, respectively.

2.2. Electronic structure calculations. Most DFT calculations were performed using Gaussian16 package,⁴⁰ with additional DFT-D computations being performed using the DFTD3 program,^(DFTD3) and depending on the availability of the functionals some DFT calculations were carried out by modified version of Gaussian03.⁴² All wave-function based calculations were carried out using MOLPRO 2012.⁴³

We obtained our reference energies for all systems from density fitting DF-MP2 computations⁴³ with a careful analysis against basis set superposition error (BSSE) and basis set incompleteness error (BSIE) for different basis sets, such as aug-cc-pVXZ⁴⁴ (namely AVXZ), with X=D, T, Q, and 5. The cohesive energies for each N water system are obtained as the difference of the cluster energy and the energies of the geometry-relaxed water monomers,

$$\Delta E_{coh} = E_{(H_2O)_{N=20,24,28,36}} - N \cdot E_{H_2O}, \quad (1)$$

while the corresponding counterpoise (CP) corrected energies were calculated by the many-body generalization of the CP correction,⁴⁵ called site-site function correction,⁴⁶ as $\Delta_{CP} = \sum_i^N (E_i^{ijkl\dots N} - E_i)$, where $E_i^{ijkl\dots N}$ are the energies for the monomers i in the basis of the N-body cluster and E_i the energies in the monomer basis computed for their geometries in the N-body cluster.

Basis set extrapolation schemes were used to reach complete basis set (CBS) limit by employ-

ing the two- and three-step formulas proposed by Schwartz⁴⁷ for the correlation energies, $E_X = E_{\text{CBS}} + \frac{A}{X^3}$, and by Peterson *et al.* for the total energies,⁴⁸ $E_X = E_{\text{CBS}} + Ae^{-(X-1)} + Be^{-(X-1)^2}$, respectively. As the CP correction has a large influence on binding and interactions energies we also employed the two-step scheme by Lee *et al.*,⁴⁹ for the interaction energies $E_{\text{CBS}} = \frac{1}{2} \frac{(\delta_X \varepsilon_{X+1} - \delta_{X+1} \varepsilon_X)}{(\delta_X - \delta_{X+1})}$, with $\delta_X = E_X^{\text{CP}} - E_X$, $\varepsilon_X = E_X^{\text{CP}} + E_X$, and E^{CP} is the CP-corrected energy, while E represents the uncorrected one, and the so-called half-counterpoise scheme,^{50,51} with the energy given as the average $\Delta E_{\text{half}} = 0.5(\Delta E_{\text{CP}} + \Delta E)$. We call the employed CBS schemes as, CBS1 the one from Ref.,⁴⁹ CBS2 from Ref.⁴⁸ and CBS3 from Ref.⁴⁷

In all DFT calculations we used both AVTZ and AVQZ basis set,⁴⁴ while DFT functionals were chosen from the different groups, such as TPSS,⁵² M06L⁵³ and the more recent developed functional SCAN⁵⁴ (meta-GGAs/third rung), B3LYP,⁵⁵ PBE0⁵⁶ and M06-2X⁵⁷ (hybrid/meta-GGAs/fourth rung), and CAMB3LYP,⁵⁸ LC- ω PBE,⁵⁹ and ω B97XD⁶⁰ (range-separated hybrid). For the numerical integration in the DFT calculations the ultrafine grid was used. In turn, we considered the dispersion corrections for the DFT and we employed the DFT-D3 correction scheme³¹ with the Becke-Johnson damping function, namely D3BJ,⁶¹ the modified D3M(BJ)³² and the D3(OP),³³ while the zero-damping D3(0) scheme was used when damping schemes are not available.

3. RESULTS AND DISCUSSION

3.1. DF-MP2 New Benchmark Energies: Comparison with Earlier Studies. The DF-MP2 interactions energies calculated with a series of correlation-consistent basis sets (AVXZ, X=T,Q, and 5) are listed in Table 1, for all the above mentioned structures with N=20, 24, 28 and 36 water molecules (see also data in the Supporting Information). Both CP corrected and uncorrected values are computed, and one can see that the CP correction counts around 20, 9, and 4.5 kcal/mol for the AVTZ, AVQZ and AV5Z basis, respectively, for the N=20 structures. By increasing the number of water molecules (from 20 to 36) the CP correction increases due to cooperative effects,

Table 1: DF-MP2 interaction energies (in kcal/mol) with, ΔE_{CP} , and without, ΔE , counterpoise correction, as well as the half-half estimate, ΔE_{half} , using AVXZ (X=T,Q,5) basis sets for all indicated structures.

Method N (Cage)	DF-MP2/AVTZ			DF-MP2/AVQZ			DF-MP2/AV5Z		
	ΔE	ΔE_{CP}	ΔE_{half}	ΔE	ΔE_{CP}	ΔE_{half}	ΔE	ΔE_{CP}	ΔE_{half}
20 (5^{12})	-186.59	-168.81	-177.70	-182.92	-174.49	-178.70	-180.67	-176.22	-178.45
20 ($4^3 5^6 6^3$)	-177.52	-159.29	-168.41	-173.99	-165.25	-169.62	-171.72	-167.11	-169.42
20 (5^{12}) ^a	-220.57	-201.76	-211.16	-217.36	-208.24	-212.80	-215.11	-210.31	-212.71
20 (ES) ^a	-227.98	-208.07	-218.02	-224.24	-214.73	-219.49	-221.79	-216.82	-219.31
20 (FC) ^a	-224.24	-204.51	-214.37	-220.48	-211.04	-215.76	-217.99	-213.09	-215.54
20 (FS) ^a	-225.78	-205.86	-215.82	-221.95	-212.43	-217.19	-219.46	-214.51	-216.99
24 ($5^{12} 6^2$)	-219.60	-197.81	-208.70	-204.87	-215.19	-210.08	-212.53	-207.06	-209.80
24 (308) ^b	-268.62	-245.55	-257.08	-264.94	-253.68	-259.31	-262.21	-256.29	-259.25
24 (316) ^b	-268.28	-245.23	-256.75	-264.62	-253.37	-258.99	-261.90	-255.98	-258.94
28 ($5^{12} 6^4$)	-265.65	-240.61	-253.13	-260.77	-248.77	-254.77	-257.58	-251.27	-254.43
36 ($5^{12} 6^8$)	-333.34	-300.69	-317.02	-327.10	-311.35	-319.23		n/a	

^a Structures from WATER27 data set.¹¹

^b Structures from Ref.³⁹

and corresponds to about 10%, 5% and 2.5% of the system binding energy for the AVTZ, AVQZ and AV5Z basis sets (see Table 1), respectively, indicating that such corrections should be taken into account for any quantitatively accurate prediction of the binding energies of these systems. Since calculations for higher-order clusters, using larger basis sets, are computationally expensive, and as we have seen the BSSE still remains, one should employ extrapolation schemes in order to obtain more accurate energy estimates. Therefore, we also list in Table 1 the calculated ΔE_{half} energies, that seem to lead to a better convergence.⁵¹

In turn, in Table 2 we list the cohesive energies obtained for all the water structures given in Fig. 1 together with their CBS limits, using all the above mentioned extrapolation schemes, CBS1, CBS2 and CBS3, as well as the corresponding ΔE_{half} values employing the AVTZ, AVQZ and AV5Z basis sets. All calculated energies are compared with best values available in the literature for each of the indicated structures. In particular, recent conventional and explicitly correlated

Table 2: DF-MP2/CBS cohesive energies (in kcal/mol) employing the indicated CBS extrapolation schemes.

N (Cage)	ΔE_{half}		CBS1 Ref. ⁴⁹		CBS2 Ref. ⁴⁸		CBS3 Ref. ⁴⁷		Best value
	AVQZ	AV5Z	[TQ]	[Q5]	[DTQ]	[TQ5]	[TQ]	[Q5]	
20 (5 ¹²)	-178.63	-178.41	-179.85	-178.17	-180.25	-177.35	-179.87	-178.56	n/a
20 (4 ³ 5 ⁶ 6 ³)	-169.55	-169.38	-170.99	-169.19	-171.19	-168.31	-170.87	-169.57	n/a
20 (5 ¹²) ^a	-199.08	-198.68	-198.94	-198.23	-199.58	-197.43	-199.91	-198.78	-199.30 ^c
20 (ES) ^a	-209.00	-208.49	-208.73	-207.95	-209.44	-207.17	-209.74	-208.54	-209.081 ^d
20 (FC) ^a	-206.70	-206.17	-206.45	-205.60	-207.16	-204.87	-207.45	-206.22	-207.534 ^d
20 (FS) ^a	-207.11	-206.59	-206.79	-206.02	-207.52	-205.26	-207.84	-206.62	-207.763 ^d
24 (5 ¹² 6 ²)	-209.99	-209.75	-211.63	-209.50	-211.93	-217.19	-211.53	-221.03	n/a
24 (308) ^b	-240.99	-240.43	-240.56	-239.81	-241.33	-248.29	-241.87	-252.49	-238.638 ^e
24 (316) ^b	-240.93	-240.36	-240.50	-239.73	-241.27	-248.22	-241.81	-252.41	-238.719 ^e
28 (5 ¹² 6 ⁴)	-254.66	-254.38	-256.62	-254.06	-256.96	-262.67	-256.45	-267.37	
36 (5 ¹² 6 ⁸)	-319.09	n/a	-321.74	n/a	-321.99	n/a	-321.38	n/a	

^a Structures from WATER27 data set.¹¹

^b Structures from Ref.³⁹

^c Best value energy from MP2-F12/A5Z' calculation.³⁵

^d Best value energies from Ref.²¹

^e Interaction energies from Ref.¹³

ab initio benchmarks have been reported for cohesive energies for four (H₂O)₂₀ structures (5^{12a}, ES^a, FC^a and FS^a) of the WATER27 data set,¹¹ at MP2-F12, MP2/CBS[56], and explicitly correlated local CCSD(T) levels of theory.^{21,35} For the 5^{12a} structure the best estimate values for the binding energy at the MP2 and CCSD(T) basis set limit reported to be³⁵ -199.3±0.2 kcal/mol, and -198.0±0.4 kcal/mol, respectively. Thus, taking into account this new best value of -199.3 kcal/mol for the dodecahedron WATER27 structure³⁵ as well as the recent values from MP2-F12 calculations²¹ for the (ES)^a, (FC)^a and (FS)^a isomers of (H₂O)₂₀ cluster (see Table 2), we plot in Fig. 2 the difference, δ , between these binding values available in the literature and the ones computed here from the DF-MP2/AV(Q,5)Z, the different DF-MP2/CBS using AVDZ up to AV5Z basis set energies, as well as the DF-MP2/AV(Q,5)Z half energy values.

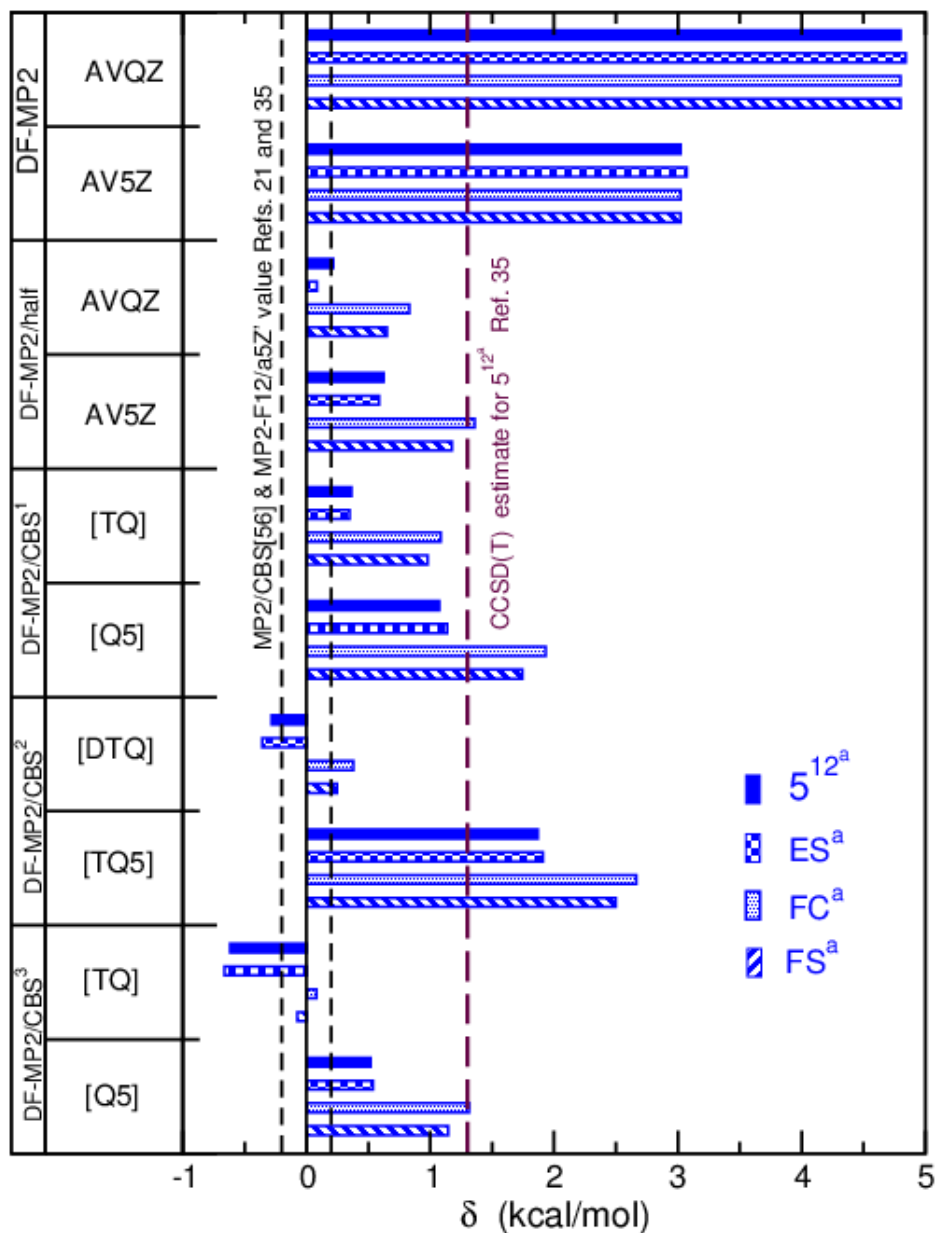


Figure 2: Comparison of DF-MP2 and DF-MP2/CBS schemes cohesive energies (in kcal/mol) of this work with the best values available from Refs.^{21,35} for the four indicated N=20 structures.¹¹ The energy difference, δ , is shown for each CBS scheme and corresponding basis sets used. Black dashed lines bracket the error of the best MP2 estimate, while color long-dashed line corresponds to the estimate of the CCSD(T) limit.

As it can be seen the DF-MP2 calculations are not converged, even with the AV5Z basis sets, although by increasing the size of the basis set the energies are found to be much closer to the best available estimates. As is expected, CBS extrapolations involving large basis sets, such as

AVQZ and AV5Z, provide better values than those using smaller, AVDZ and AVTZ, basis. Taking into account the errors reported for the MP2 limit value (-199.3 ± 0.2 kcal/mol),³⁵ shown by the black dashed lines in Fig. 2, as well as the reported CCSD(T) limit value (see color long-dashed line in Fig. 2), we consider that both DF-MP2/CBS1[TQ] and DF-MP2/CBS1[Q5], and the DF-MP2/CBS2[TQ5] schemes as well as the DF-MP2/AV5Z half energy values show a consistent behavior as a function of the size of the basis set used. So, given that for the higher-order, N=36, water structure, we only could obtain interaction/cohesive energies with the AVQZ basis set, we then choose as the reference values for the binding energies in this work the DF-MP2/CBS1[Q5] for all N=20-28 water clusters, and the DF-MP2/CBS1[TQ] for the N=36 structure. One can see, in Table 2, that these cohesive energies are -198.23 kcal/mol for the 5^{12a} , just 0.23 kcal/mol to the previous reported CCSD(T) limit,³⁵ -178.17 and -169.19 kcal/mol for the 5^{12} and the $4^3 5^6 6^3$, respectively, -209.50 kcal/mol for the $5^{12} 6^2$, -254.06 kcal/mol for the $5^{12} 6^4$, and -321.74 kcal/mol for the $5^{12} 6^8$ cages.

3.2. Water Model Potentials: Pairwise and Many-Body effects. Over a hundred different water models⁶²⁻⁶⁴ are available in the literature since the first attempt by Bernal-Fowler in 1933. A general classification could be made by the degree of their complexity. For example, water models could be pairwise additive (two-body) or polarizable (many-body) that treat explicitly many-body inductive effects, and also rigid or flexible depending on whether the model includes deformation of the monomers. By combining the above groups we can obtain categories of water models with increasing degree of complexity, with the majority of the existing models being: rigid-pairwise, rigid-polarizable, flexible-pairwise, and flexible-polarizable. Apart such models could be classified based on the origin of the data used for its parameterization to semiempirical or *ab initio*. Semiempirical models have been adjusted to describe properties of the system at specific thermodynamic conditions. Among them, we employed here, three of the most popular semiempirical waters models, namely TIP4P/ice, TIP4P/2005 and the flexible q-TIP4P/F.⁶⁵⁻⁶⁷ On the other hand, *ab initio* potentials are usually designed to account for the complex short-range interactions, and the subtle weak (long-range) interactions by fits to huge datasets of electronic structure calculations of the

system including pairwise and some of them explicit higher-order many-body contributions (up to three-body ones). Here, we choose recent Thole-type flexible-polarizable *ab initio* potentials reported in the literature, called TTM2-F, TTM3-F, TTM4-F and MB-pol.^{68–71}

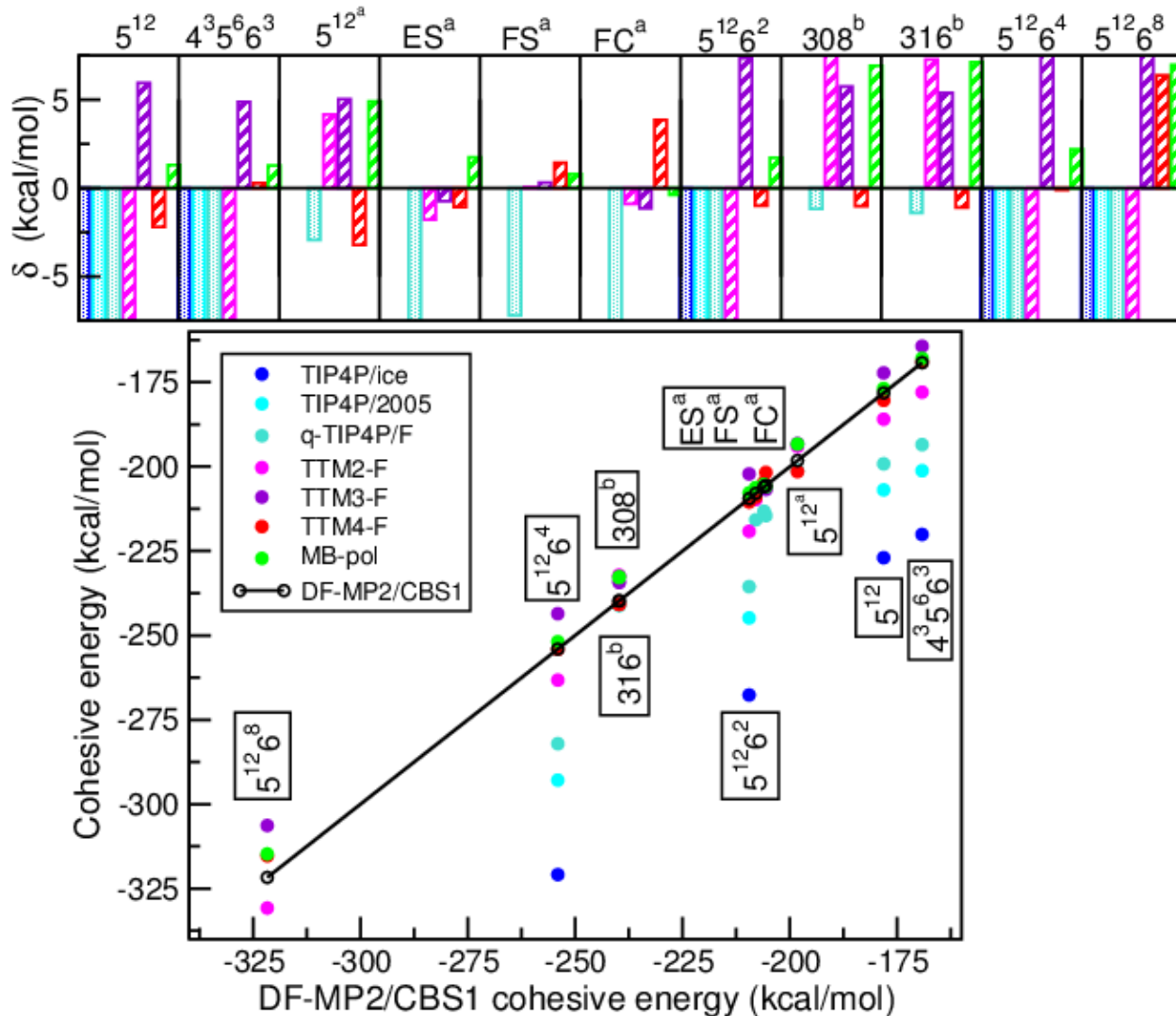


Figure 3: Cohesive energies obtained from the indicated analytical semiempirical or *ab initio*-based water potentials, and their comparison with the corresponding DF-MP2/CBS1 values. Total energies are shown in the lower panel, while their difference, δ , from the DF-MP2/CBS1 ones are given in the upper panel for each water structure/cavity.

In Fig. 3 (see lower panel) we show correlation plots of the DF-MP2/CBS1 and different water model cohesive energies for each structure or clathrate cavity, while in the upper panel we plot the obtained differences of each water model potential and structure from the corresponding DF-MP2/CBS1 reference energy value. We should point out that comparisons for the semiempirical

TIP4P/ice and TIP4P/2005 models are only presented here for those five structures that the water monomers are fixed, while for the flexible semiempirical q-TIP4P/F and the *ab initio*-based TTM2-F, TTM3-F, TTM4-F, and MB-pol potentials comparisons are shown for all structures. As it can be seen, all semiempirical models fails to predict the energetics of such water clusters, while *ab initio*-based water models seem to provide estimates closer to the reference values. In general, we found that the TTM3-F, TTM4-F and MB-pol models show somehow similar behavior, with the TTM4-F and MB-pol having smaller errors in the case of the smaller water cavities. We should note that the MB-pol model incorporates short-range three-body terms by fitting to CCSD(T) water trimer energies, while higher-body effects described by induction as in the TTM4-F model, so one should expect that it should perform better than the models with only pair short-range components in describing cooperative many-body effects in such systems.

3.3. Comparative Analysis of DFT/DFT-D Approaches. As we mentioned above we choose

Table 3: Cohesive energies from DFT and DFT-D3 calculations using the indicated functionals, basis sets and D3 dispersion corrections for the 5^{12a} structure.

Basis set/ Functional	AVTZ	AVQZ	ΔE_{basis}	D3 dispersion		
				(BJ)	M(BJ)	(OP)
TPSS	-190.94	-188.82	-2.12	-23.80	n/a	-21.70
SCAN	-220.21	-225.53	5.32	-7.55	n/a	n/a
M06L	-190.86	-188.63	-2.23	-4.51*		
B3LYP	-185.33	-184.32	-1.01	-28.58	-30.67	-23.25
PBE0	-200.84	-199.47	-1.37	-17.65	-17.51	-14.47
M06-2X	-202.44	-200.61	-1.83	-4.00*		
CAM-B3LYP	-209.53	-208.36	-1.17	-16.23	n/a	n/a
LC- ω PBE	-180.11	-179.23	-0.88	-18.63	n/a	n/a
ω B97XD	-203.94	-200.46	-3.47	n/a	n/a	n/a

* This value corresponds to D3(0) correction.

different DFT functionals in the present study: as a first example, three meta-GGAs functionals, TPSS, M06L and SCAN, then three popular hybrid functionals (B3LYP, PBE0, and M06-2X), and as a final example, three long-range-corrected functionals, CAM-B3LYP, LC- ω PBE, and ω B97XD (that includes the D2 correction). In Table 3 the calculated energies are compared for the 5^{12a} structure using the AVTZ and AVQZ basis sets and the D3(BJ), D3M(BJ) and D3(OP)

damping schemes, while the D3(0) scheme is used in the case where damping schemes are not available. Energies for all 11 water structures discussed in this study from the DFT and DFT-D3 calculations are listed in the Supporting Information.

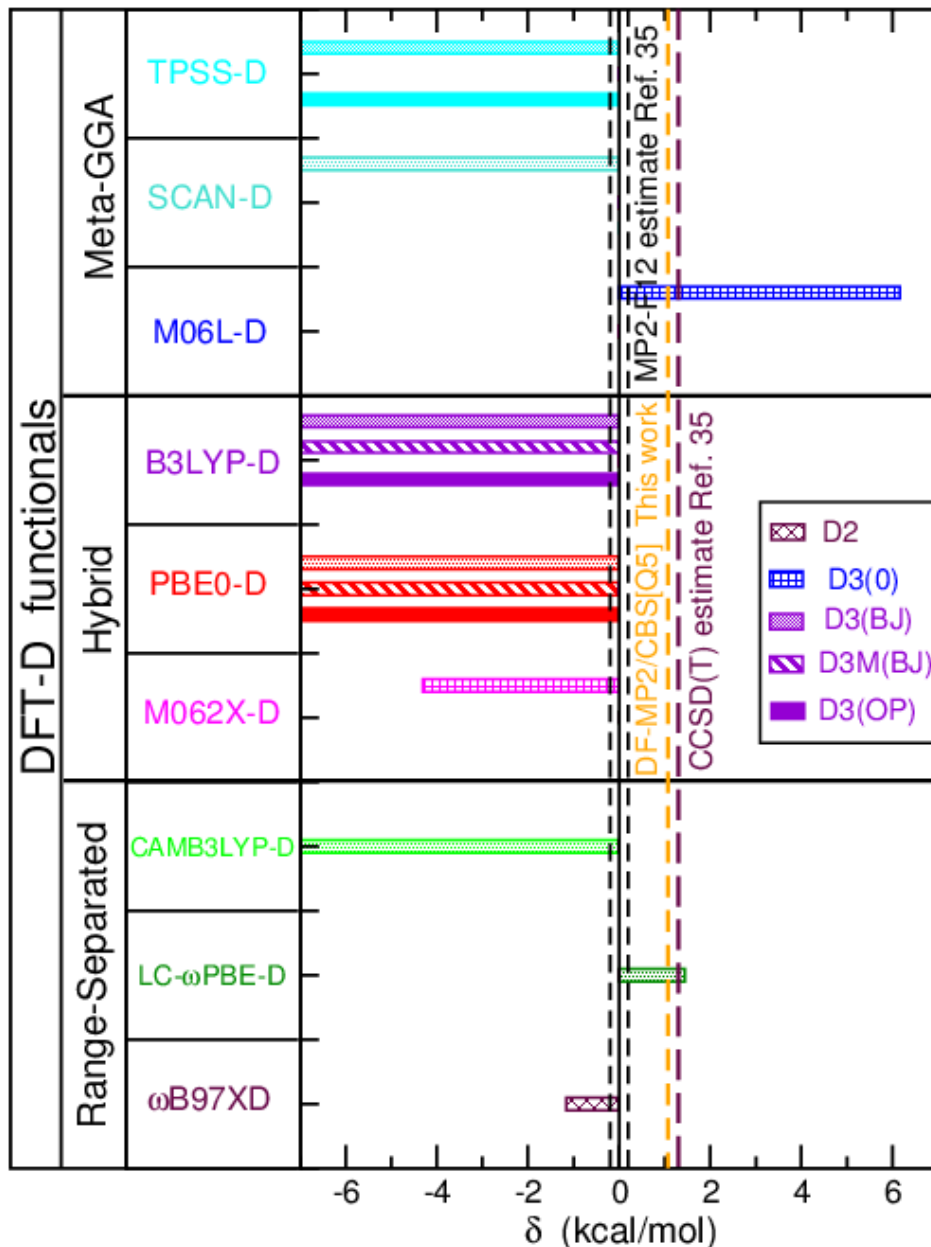


Figure 4: Cohesive energy difference, δ , for the 5^{12a} structure obtained from the indicated DFT-D calculations from the reference value from Ref. ³⁵

On the one hand, one can see the effect of the basis set used for each functional, that contribute from -0.88 to 5.32 kcal/mol to the energy values, and on the other hand, the contribution of the

dispersion correction that ranges from -7.55 up to -30.67 kcal/mol depending mainly on the type of damping used in the D3 scheme, while it counts around -4.0 kcal/mol for the D3(0) correction.

For evaluating the performance of each functional, as a first step, we compare (see Fig. 4) the cohesive energy values calculated from the DFT-D functionals with the reference MP2-F12 value of -199.3 ± 0.2 kcal/mol (black dashed lines correspond to the estimate errors) available in the literature³⁵ for the dodecahedron 5^{12a} structure. We also indicated the CCSD(T) estimate³⁵ (see color long-dashed line), as well as the value obtained here from the DF-MP2/CBS1 calculations (see orange-color long-dashed line). As it can be seen, meta-GGAs and hybrid functionals show difficulties to determine the cohesive energy of the dodecahedron structure, presenting large errors (more than 5 kcal/mol), while the LC- ω PBE functional including the D3(BJ) dispersion correction shows the best performance for this water cage structure.

Thus, in a next step in order to evaluate the performance of the DFT functionals as a function of the cage size and type, in Fig. 5 we present additional error bar plots for the remaining 5^{12} , $4^3 5^6 6^3$, 5^{12} , $5^{12} 6^2$, $5^{12} 6^4$ and $5^{12} 6^8$ clathrate cages containing 20, 20, 24, 28 and 36 water molecules, respectively. DFT calculations were carried out using the AVQZ basis for all structures with $N=20$, and the AVTZ for all other structures. Now the comparison is made with respect the above reported DF-MP2/CBS1 energies (see Table 2) for each structure, where one can observe some clear trends in the performance of each functional. In particular, all functionals, except the M06L-D3(0) and LC- ω PBE-D3(BJ) ones, overestimate the binding energy of all cages, with TPSS-D3(OP), B3LYP-D3(OP), M062X-D3(0) and ω B97XD providing closer values, while others show much higher deviations. The M06-2X functional without any dispersion corrections seems to outperform all other functionals, predicting the lowest error respect to the benchmark energies for all structures. As in the case of the 5^{12a} structure (see Fig. 4) the M06L-D3(0) and the LC- ω PBE-D3(BJ) functionals consistently underpredict the intermolecular interactions for all cages, and by including D3 dispersion correction one can see that their results are improved. Although, relatively low errors are found for the $N=20$, 24 and 28 water cages, both the M06L-D3(0) and LC- ω PBE-D3(BJ) functionals cannot predict quantitative accurate results for the binding energy of the largest, $N=36$,

clathrate cage. However, we should point out that in the N=36 case the reference energy value is based on the DF-MP2/CBS1[TQ] limit (see Table 2), and this could probably also contribute to the error.

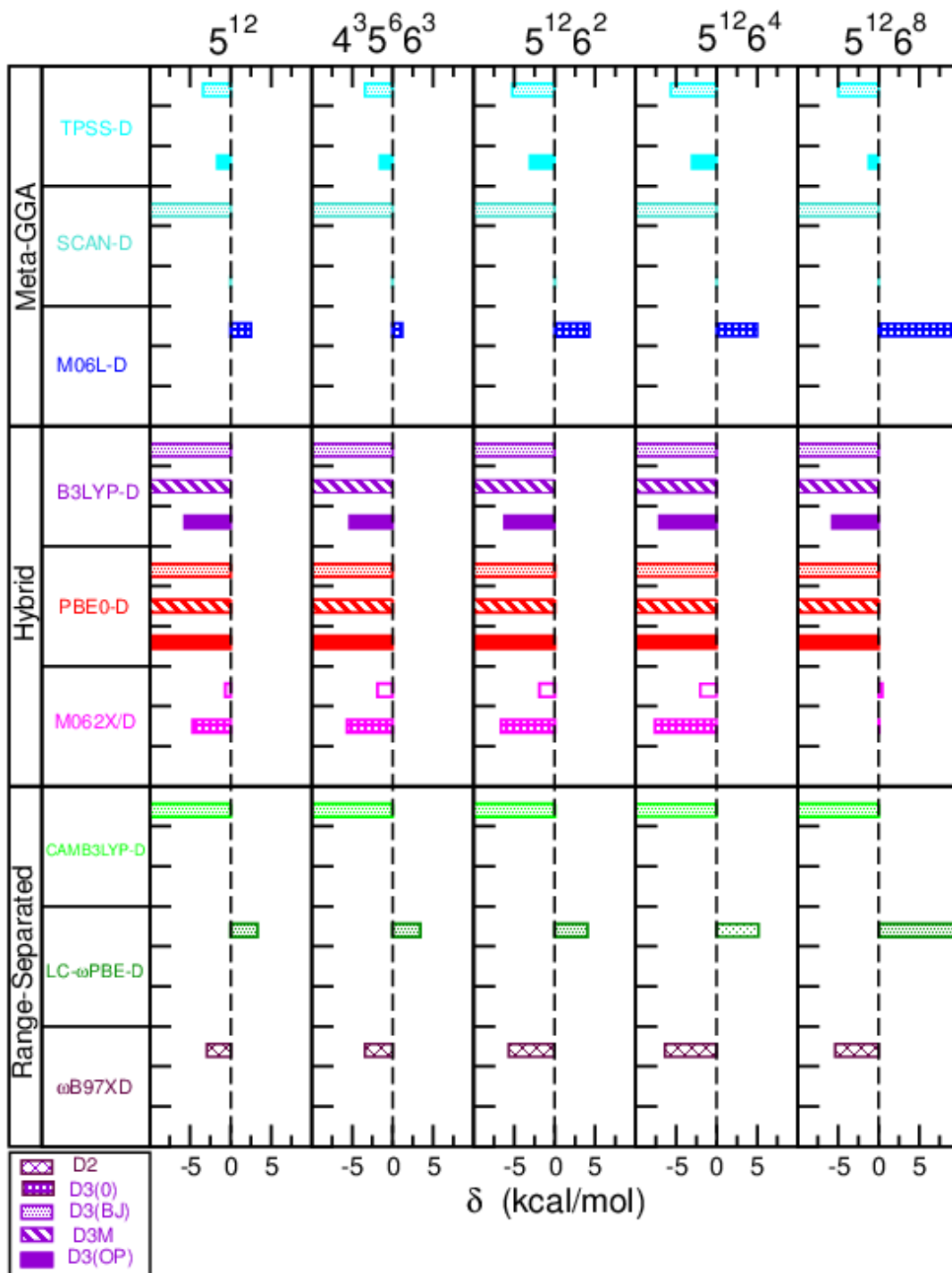


Figure 5: Cohesive energy difference, δ , for the indicated cage structures obtained from the DFT calculations and the reference DF-MP2/CBS1 values.

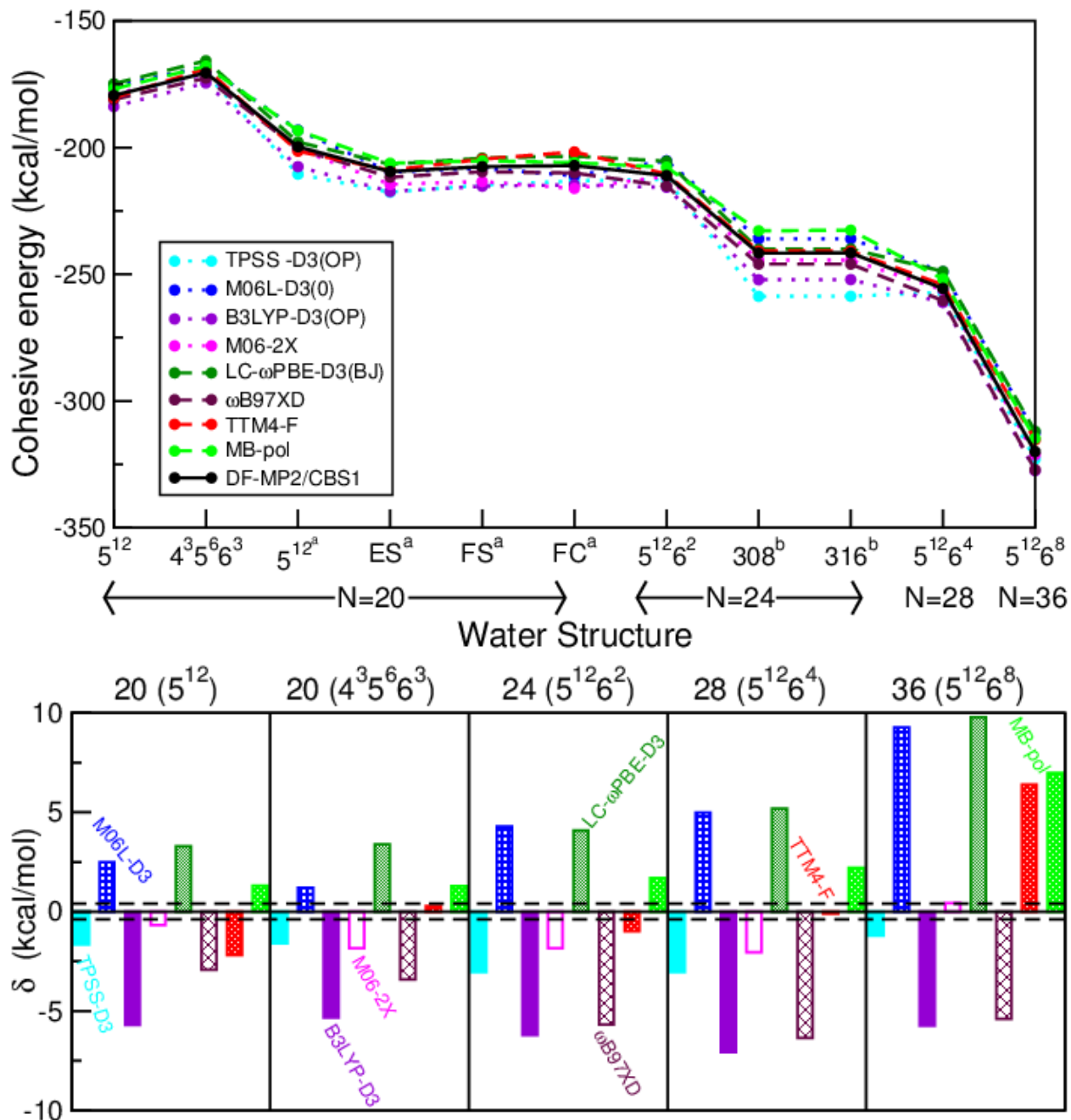


Figure 6: Cohesive energies obtained from the best-performed DFT functionals and *ab initio* water models with respect to the reference DF-MP2/CBS1 values for the indicated water structures and clathrate cages.

Finally, in Fig. 6 (see upper panel) we summarized the estimates of the binding energies of all structures, as they predicted by the "best"-performed DFT functionals as well as the most accurate analytical water models available in comparison with the benchmark DF-MP2/CBS1 values

of this work. Specifically, we show the energies for two meta-GGAs (the TTPS-D3(OP) and M06L-D3(0)), two hybrids with and without dispersion correction, B3LYP-D3(OP) and M06-2X, respectively, and two range-separated, ω B97XD and LC- ω PBE-D3(BJ), functionals, as well as for the *ab initio*-based Thole-type water potentials, TTM4-F and MB-pol. One can see that both best-performed DFT functionals (M06L-D3(0), M06-2X, and LC- ω PBE-D3(BJ)) and water model potentials show a very similar behavior as a function of the structure and the number of water molecules. In the lower panel of Fig. 6 we display deviations obtained for each water cage structure, and we found that smaller deviations are obtained for the M06-2X, even for the N=36 structure where both M06L-D3(0) and LC- ω PBE-D3(BJ) DFT approaches and *ab initio*-based models show larger differences.

4. SUMMARY AND CONCLUSIONS

We have assessed the performance of a variety of DFT-based methods and few of the most used semiempirical and *ab initio*-based water models by comparisons with reference data obtained from wave-function based methods for specific guest-free clathrate-like cavities. Totally eleven structures formed by N=20, 24, 28 and 36 water molecules were used to calculate binding energies, and new, converged, benchmark energies at DF-MP2/CBS level of theory are reported for all cages of the sI, sII and sH clathrates. We should notice that such water systems suffer from huge BSSE, even in large (*e.g.* AV5Z) basis sets, and thus extrapolation schemes were used to obtain more accurate results. These data were then used to evaluate the performance of the DFT approaches. In particular we employed meta-GGAs, hybrids and range-separated functionals. As dispersion contributes to the correct description of noncovalent interactions, we also checked here the dispersion corrections, employing recent damping functions within the DFT-D3 semiempirical scheme. Among the studied water models and DFT functionals we found difficulties in describing accurately such water systems. However, *ab initio*-based potentials, such as TTM4-F and MB-pol, show relatively satisfactory description of the energies of the smaller clusters, while DFT functionals, within dif-

ferent Jacob's rungs, like the M06L-D3(0), the M06-2X and the LC- ω PBE-D3(BJ) ones, provide the best estimates of the cohesive energies for all water structures studied. Thus, one may conclude that substantial many-body errors are still present for such molecular systems, and further explicit investigation of such errors should be carried out including a broader range of improved dispersion-corrected functionals. Finally, we should emphasize that benchmark electronic structure calculations are the key point in assessing DFT approaches and model potentials for clusters, providing valuable information to improve upon the existing approaches or develop new ones for describing larger-size or condensed-phase systems.

Acknowledgement

The authors thanks Dr. Jianwei Sun for providing the source code of the SCAN functional. The authors thank to Centro de Calculo del IFF, SGAI (CSIC) and CESGA for allocation of computer time. This work has been supported by MINECO grants No. FIS2014-51933-P and FIS2017-83157-P, and COST Action CM1405(MOLIM). I.L.M. acknowledges CSIC for a JAE-Intro-2017 fellowship, Ref:JAEINT17_EX_0020.

Supporting Information Available

Cartesian coordinates of 5^{12} , $4^3 5^6 6^3$, $5^{12} 6^2$, $5^{12} 6^4$ and $5^{12} 6^8$ structures.

DF-MP2 total, interaction and cohesive energies for all water structures studied in this work.

DFT and DFT-D3 total and cohesive energies for all water structures discussed in the study. This material is available free of charge via the Internet at <http://pubs.acs.org/>.

References

- (1) Sloan, E. D.; Koh, C. A. *Clathrate Hydrates of Natural Gasess*, 3rd ed.; CRC Press, 2007.
- (2) Ripmeester, J. A.; Alavi, S. Some current challenges in clathrate hydrate science: Nucleation, decomposition and the memory effect. *Curr. Opin. Solid ST. M.* **2016**, *20*, 344 – 351.

- (3) Jacobson, L. C.; Molinero, V. A Methane-Water Model for Coarse-Grained Simulations of Solutions and Clathrate Hydrates. *J. Phys. Chem. B* **2010**, *114*, 7302–7311.
- (4) Falenty, A.; Hansen, T. C.; Kuhs, W. F. Formation and properties of ice XVI obtained by emptying a type sII clathrate hydrate. *Nature Lett.* **2014**, *516*, 231 – 233.
- (5) Huang, Y.; Zhu, C.; Wang, L.; Cao, X.; Su, Y.; Jiang, X.; Meng, S.; Zhao, J.; Zeng, X. C. A new phase diagram of water under negative pressure: The rise of the lowest-density clathrate s-III. *Sci. Adv.* **2016**, *2*, e1501010 .
- (6) Conde, M. M.; Vega, C.; Tribello, G. A.; Slater, B. The phase diagram of water at negative pressures: Virtual ices. *J. Chem. Phys.* **2009**, *131*, 034510.
- (7) Matsui, T.; Hirata, M.; Yagasaki, T.; Matsumoto, M.; Tanaka, H. Communication: Hypothetical ultralow-density ice polymorphs. *J. Chem. Phys.* **2017**, *147*, 091101.
- (8) Valdés, A.; Arismendi-Arrieta, D. J.; Prosmi, R. Quantum Dynamics of Carbon Dioxide Encapsulated in the Cages of the sI Clathrate Hydrate: Structural Guest Distributions and Cage Occupation. *J. Phys. Chem. C* **2015**, *119*, 3945–3956.
- (9) Vitek, A.; Arismendi-Arrieta, D. J.; Rodriguez-Cantano, R.; Prosmi, R.; Villarreal, P.; Kalus, R.; Delgado-Barrio, G. Computational investigations of the thermodynamic properties of size-selected water and Ar-water clusters: high-pressure transitions. *Phys. Chem. Chem. Phys.* **2015**, *17*, 8792–8801.
- (10) Arismendi-Arrieta, D. J.; Vitek, A.; Prosmi, R. High Pressure Structural Transitions in Kr Clathrate-Like Clusters. *J. Phys. Chem. C* **2016**, *120*, 26093–26102.
- (11) Bryantsev, V. S.; Diallo, M. S.; van Duin, A. C. T.; Goddard, W. A. Evaluation of B3LYP, X3LYP, and M06-Class Density Functionals for Predicting the Binding Energies of Neutral, Protonated, and Deprotonated Water Clusters. *J. Chem. Theory Comput.* **2009**, *5*, 1016–1026.

- (12) Yoo, S.; Kirov, M. V.; Xantheas, S. S. Low-Energy Networks of the T-Cage (H₂O)₂₄ Cluster and Their Use in Constructing Periodic Unit Cells of the Structure I (sI) Hydrate Lattice. *J. Am. Chem. Soc.* **2009**, *131*, 7564–7566.
- (13) Góra, U.; Podeszwa, R.; Cencek, W.; Szalewicz, K. Interaction energies of large clusters from many-body expansion. *J. Chem. Phys.* **2011**, *135*, 224102.
- (14) Yoo, S.; Xantheas, S. S. In *Handbook of Computational Chemistry*; Leszczynski, J., Ed.; Springer Netherlands: Dordrecht, 2012; pp 761–792.
- (15) Wang, K.; Li, W.; Li, S. Generalized Energy-Based Fragmentation CCSD(T)-F12a Method and Application to the Relative Energies of Water Clusters (H₂O)₂₀. *J. Chem. Theory Comput.* **2014**, *10*, 1546–1553.
- (16) Anacker, T.; Friedrich, J. New accurate benchmark energies for large water clusters: DFT is better than expected. *J. Comput. Chem.* **2014**, *35*, 634–643.
- (17) Miliordos, E.; Xantheas, S. S. An accurate and efficient computational protocol for obtaining the complete basis set limits of the binding energies of water clusters at the MP2 and CCSD(T) levels of theory: Application to (H₂O)_m, m = 2-6, 8, 11, 16, and 17. *J. Chem. Phys.* **2015**, *142*, 234303.
- (18) Mezei, P. D.; Ruzsinszky, A.; Csonka, G. I. Application of a Dual-Hybrid Direct Random Phase Approximation to Water Clusters. *J. Chem. Theory Comput.* **2016**, *12*, 4222–4232.
- (19) Gillan, M. J.; Alfé, D.; Michaelides, A. Perspective: How good is DFT for water? *J. Chem. Phys.* **2016**, *144*, 130901.
- (20) Jordan, K. D.; Sen, K. *Chemical Modelling: Volume 13*; The Royal Society of Chemistry, 2017; pp 105–131.

- (21) Manna, D.; Kesharwani, M. K.; Sylvetsky, N.; Martin, J. M. L. Conventional and Explicitly Correlated ab Initio Benchmark Study on Water Clusters: Revision of the BEGDB and WATER27 Data Sets. *J. Chem. Theory Comput.* **2017**, *13*, 3136–3152.
- (22) Deible, M. J.; Tuguldur, O.; Jordan, K. D. Theoretical Study of the Binding Energy of a Methane Molecule in a (H₂O)₂₀ Dodecahedral Cage. *J. Phys. Chem. B* **2014**, *118*, 8257–8263.
- (23) Sun, N.; Li, Z.; Qiu, N.; Yu, X.; Zhang, X.; Li, Y.; Yang, L.; Luo, K.; Huang, Q.; Du, S. Ab Initio Studies on the Clathrate Hydrates of Some Nitrogen- and Sulfur-Containing Gases. *J. Phys. Chem. A* **2017**, *121*, 2620–2626.
- (24) Riley, K. E.; Pitonák, M.; Jurecka, P.; Hobza, P. Stabilization and Structure Calculations for Noncovalent Interactions in Extended Molecular Systems Based on Wave Function and Density Functional Theories. *Chem. Rev.* **2010**, *110*, 5023–5063.
- (25) Medvedev, M. G.; Bushmarinov, I. S.; Sun, J.; Perdew, J. P.; Lyssenko, K. A. Density functional theory is straying from the path toward the exact functional. *Science* **2017**, *355*, 49–52.
- (26) Johnson, E. R.; Mackie, I. D.; DiLabio, G. A. Dispersion interactions in density-functional theory. *J. Phys. Org. Chem.* **2009**, *22*, 1127–1135.
- (27) Grimme, S. Density functional theory with London dispersion corrections. *WIREs: Comput. Mol. Sci.* **2011**, *1*, 211–228.
- (28) Tkatchenko, A.; Romaner, L.; Hofmann, O. T.; Zojer, E.; Ambrosch-Draxl, C.; Scheffler, M. Van der Waals Interactions Between Organic Adsorbates and at Organic/Inorganic Interfaces. *MRS Bull.* **2010**, *35*, 435–442.
- (29) Vydrov, O. A.; Voorhis, T. V. In *Fundamentals of Time-Dependent Density Functional Theory*; Marques, M., Maitra, N., Nogueira, F., Gross, E., Rubio, A., Eds.; Springer-Verlag: Berlin Heidelberg, 2012; pp 443–456.

- (30) Klimes, J.; Michaelides, A. Perspective: Advances and challenges in treating van der Waals dispersion forces in density functional theory. *J. Chem. Phys.* **2012**, *137*, 120901.
- (31) Grimme, S.; Antony, J.; Ehrlich, S.; Krieg, H. A consistent and accurate ab initio parametrization of density functional dispersion correction (DFT-D) for the 94 elements H-Pu. *J. Chem. Phys.* **2010**, *132*, 154104.
- (32) Smith, D. G. A.; Burns, L. A.; Patkowski, K.; Sherrill, C. D. Revised Damping Parameters for the D3 Dispersion Correction to Density Functional Theory. *J. Phys. Chem. Lett.* **2016**, *7*, 2197–2203.
- (33) Witte, J.; Mardirossian, N.; Neaton, J. B.; Head-Gordon, M. Assessing DFT-D3 Damping Functions Across Widely Used Density Functionals: Can We Do Better? *J. Chem. Theory Comput.* **2017**, *13*, 2043–2052.
- (34) Alcami, M.; Mo, O.; Yanez, M.; Alkorta, I.; Elguero, J. Triaziridine and tetrazetidine vs. cyclic water trimer and tetramer: A computational approach to the relationship between molecular and supramolecular conformational analysis. *Phys. Chem. Chem. Phys.* **2002**, *4*, 2123–2129.
- (35) Schmitz, G.; Hättig, C. Accuracy of Explicitly Correlated Local PNO-CCSD(T). *J. Chem. Theory Comput.* **2017**, *13*, 2623–2633.
- (36) Viegas, L. P.; Varandas, A. J. C. Role of $(\text{H}_2\text{O})_n$ ($n = 2-3$) Clusters on the $\text{HO}_2 + \text{O}_3$ Reaction: A Theoretical Study. *J. Phys. Chem. B* **2016**, *120*, 1560–1568.
- (37) Takeuchi, F.; Hiratsuka, M.; Ohmura, R.; Alavi, S.; Sum, A.; Yasuoka, K. Water proton configurations in structures I, II, and H clathrate hydrate unit cells. *J. Chem. Phys.* **2013**, *138*, 124504.
- (38) Wales, D. J.; Hodges, M. P. Global minima of water clusters $(\text{H}_2\text{O})_n$, $n < 21$, described by an empirical potential. *Chem. Phys. Lett.* **1998**, *286*, 65 – 72.

- (39) Aprà, E.; Rendell, A. P.; Harrison, R. J.; Tipparaju, V.; deJong, W. A.; Xantheas, S. S. Liquid Water: Obtaining the Right Answer for the Right Reasons, Proceedings of the Conference on High Performance Computing Networking, Storage and Analysis, Portland, Oregon, 2009; ACM:New York, NY, USA, 2009.
- (40) Frisch, M. J.; Trucks, G. W.; Schlegel, H. B.; Scuseria, G. E.; Robb, M. A.; Cheeseman, J. R.; Scalmani, G.; Barone, V.; Mennucci, B.; Petersson, G. A. et al. Gaussian 16 Revision A.03. 2016; Gaussian Inc. Wallingford CT.
- (DFTD3)) DFT-D3 - A dispersion correction for density functionals, Hartree-Fock and semi-empirical quantum chemical methods DFT-D3. 2017; <https://www.chemie.uni-bonn.de/pctc/mulliken-center/software/dft-d3>.
- (42) Frisch, M. J.; Trucks, G. W.; Schlegel, H. B.; Scuseria, G. E.; Robb, M. A.; Cheeseman, J. R.; Montgomery, J. A., Jr.; Vreven, T.; Kudin, K. N.; Burant, J. C. et al. Gaussian 03, Revision C.02. Gaussian, Inc., Wallingford, CT, 2004.
- (43) Werner, H.-J.; Knowles, P. J.; Knizia, G.; Manby, F. R.; M. Schütz, M.; et al., MOLPRO, Version 2012.1, A Package of Ab Initio Programs. See <http://www.molpro.net>.
- (44) Kendall, R. A.; Jr., T. H. D.; Harrison, R. J. Electron affinities of the first-row atoms revisited. Systematic basis sets and wave functions. *J. Chem. Phys.* **1992**, *96*, 6796–6806.
- (45) Boys, S.; Bernardi, F. The calculation of small molecular interactions by the differences of separate total energies. Some procedures with reduced errors. *Mol. Phys.* **1970**, *19*, 553–566.
- (46) Wells, B. H.; Wilson, S. van der Waals interaction potentials: Many-body basis set superposition effects. *Chem. Phys. Lett.* **1983**, *101*, 429 – 434.
- (47) Schwartz, C. Importance of Angular Correlations between Atomic Electrons. *Phys. Rev.* **1962**, *126*, 1015–1019.

- (48) Peterson, K. A.; Woon, D. E.; Jr., T. H. D. Benchmark calculations with correlated molecular wave functions. IV. The classical barrier height of the $\text{H}+\text{H}_2\rightarrow\text{H}_2+\text{H}$ reaction. *J. Chem. Phys.* **1994**, *100*, 7410–7415.
- (49) Lee, E. C.; Kim, D.; Jurecka, P.; Tarakeshwar, P.; Hobza, P.; Kim, K. S. Understanding of Assembly Phenomena by Aromatic-Aromatic Interactions: Benzene Dimer and the Substituted Systems. *J. Phys. Chem. A* **2007**, *111*, 3446–3457.
- (50) Halkier, A.; Klopper, W.; Helgaker, T.; Jørgensen, P.; Taylor, P. R. Basis set convergence of the interaction energy of hydrogen-bonded complexes. *J. Chem. Phys.* **1999**, *111*, 9157–9167.
- (51) Burns, L.; Marshall, M.; Sherrill, C. Comparing Counterpoise-Corrected, Uncorrected, and Averaged Binding Energies for Benchmarking Noncovalent Interactions. *J. Chem. Theory Comput.* **2014**, *10*, 49–57.
- (52) Tao, J.; Perdew, J. P.; Staroverov, V. N.; Scuseria, G. E. Climbing the Density Functional Ladder: Nonempirical Meta-Generalized Gradient Approximation Designed for Molecules and Solids. *Phys. Rev. Lett.* **2003**, *91*, 146401.
- (53) Zhao, Y.; Truhlar, D. G. A new local density functional for main-group thermochemistry, transition metal bonding, thermochemical kinetics, and noncovalent interactions. *J. Chem. Phys.* **2006**, *125*, 194101.
- (54) Sun, J.; Remsing, R. C.; Zhang, Y.; Sun, Z.; Ruzsinszky, A.; Peng, H.; Yang, Z.; Paul, A.; Waghmare, U.; Wu, X. et al. Accurate first-principles structures and energies of diversely bonded systems from an efficient density functional. *Nat. Chem.* **2016**, *8*, 831–836.
- (55) Becke, A. D. Density-functional thermochemistry. III. The role of exact exchange. *J. Chem. Phys.* **1993**, *98*, 5648–5652.

- (56) Adamo, C.; Barone, V. Toward reliable density functional methods without adjustable parameters: The PBE0 model. *J. Chem. Phys.* **1999**, *110*, 6158–6170.
- (57) Zhao, Y.; Truhlar, D. G. The M06 suite of density functionals for main group thermochemistry, thermochemical kinetics, noncovalent interactions, excited states, and transition elements: two new functionals and systematic testing of four M06-class functionals and 12 other functionals. *Theor. Chem. Acc.* **2008**, *120*, 215–241.
- (58) Yanai, T.; Tew, D. P.; Handy, N. C. A new hybrid exchange-correlation functional using the Coulomb-attenuating method (CAM-B3LYP). *Chem. Phys. Lett.* **2004**, *393*, 51 – 57.
- (59) Vydrov, O. A.; Scuseria, G. E. Assessment of a long-range corrected hybrid functional. *J. Chem. Phys.* **2006**, *125*, 234109.
- (60) Chai, J.-D.; Head-Gordon, M. Systematic optimization of long-range corrected hybrid density functionals. *J. Chem. Phys.* **2008**, *128*, 084106.
- (61) Grimme, E.; Ehrlich, S.; Goerigk, L. Effect of the Damping Function in Dispersion Corrected Density Functional Theory. *J. Comput. Chem.* **2011**, *32*, 1456–1465.
- (62) Vega, C.; Abascal, J. Simulating water with rigid non-polarizable models: a general perspective. *Phys. Chem. Chem. Phys.* **2011**, *13*, 19663–19688.
- (63) Ouyang, J.; Bettens, R. Modelling Water: A Lifetime Enigma. *CHIMIA Inter. J. Chem.* **2015**, *69*, 104–111.
- (64) Cisneros, G. A.; Wikfeldt, K.; Ojamäe, L.; Lu, J.; Xu, Y.; Torabifard, H.; Bartók, A.; Csányi, G.; Molinero, V.; Paesani, F. Modeling Molecular Interactions in Water: From Pairwise to Many-Body Potential Energy Functions. *Chem. Rev.* **2016**, *116*, 7501–7528.
- (65) Abascal, J.; Sanz, E.; Fernández, R. G.; Vega, C. A potential model for the study of ices and amorphous water: TIP4P/Ice. *J. Chem. Phys.* **2005**, *122*, 234511.

- (66) Abascal, J. L. F.; Vega, C. A general purpose model for the condensed phases of water: TIP4P/2005. *J. Chem. Phys.* **2005**, *123*, 234505.
- (67) Habershon, S.; Markland, T. E.; Manolopoulos, D. E. Competing quantum effects in the dynamics of a flexible water model. *J. Chem. Phys.* **2009**, *131*, 024501.
- (68) Fanourgakis, G.; Xantheas, S. The flexible, polarizable, thole-type interaction potential for water (TTM2-F) revisited. *J. Phys. Chem. A* **2006**, *110*, 4100–4106.
- (69) Fanourgakis, G.; Xantheas, S. Development of transferable interaction potentials for water. V. Extension of the flexible, polarizable, Thole-type model potential (TTM3-F, v. 3.0) to describe the vibrational spectra of water clusters and liquid water. *J. Chem. Phys.* **2008**, *128*, 074506.
- (70) Burnham, C. J.; Anick, D. J.; Mankoo, P. K.; Reiter, G. F. The Vibrational Proton Potential in Bulk Liquid Water and Ice. *J. Chem. Phys.* **2008**, *128*, 154519.
- (71) Babin, V.; Leforestier, C.; Paesani, F. Development of a “First Principles” Water Potential with Flexible Monomers: Dimer Potential Energy Surface, VRT Spectrum, and Second Virial Coefficient. *J. Chem. Theory Comput.* **2013**, *9*, 5395–5403.

TOC Graphic

